Biophysical Chemistry 22 (1985) 219–235
Elsevier

BPC 01009

THE BIOLOGICAL FUNCTIONS OF LOW-FREQUENCY VIBRATIONS (PHONONS)

5. A PHENOMENOLOGICAL THEORY *

Kuo-Chen CHOU [a] and Yuan-Sun KIANG [b,**]

[a] *Baker Laboratory of Chemistry, Cornell University, Ithaca, NY 14853, U.S.A. and* [b] *Institute of Theoretical Chemistry, Jilin University, Changchun, China*

Received 18th June 1984
Revised manuscript received 22nd January 1985
Accepted 21st May 1985

Key words: Low-frequency resonance; Energy transmission; Cooperativity Resonance-controlled trigger; Allosteric transition

Low-frequency internal motions of a biomacromolecule are thought to possess significant biological function from the dynamic point of view. In this paper, a general phenomenological theory is established by which it is clearly verified that low-frequency resonance plays a central role in the energy transmission required during the cooperative interaction between subunits in a protein oligomer. According to the present theory, it is found that the energy transmission between a pair of diagonal subunits in a protein oligomer with a polygon arrangement is the most efficient, so as to in a sense further predict that after a ligand is bound to a subunit by random collision, its diagonal subunit in the same protein oligomer will possess the greatest probability of binding with the next ligand. Furthermore, based on the concept of the 'resonance-controlled trigger' derived from the phenomenological theory, it is feasible to estimate the lower time limit of allosteric transition from one subunit to the other. Such a time limit depends on the dominant low-frequency mode of each subunit, the ratio of the coupling force constant to the corresponding inherent force constant, as well as the geometrical arrangement of subunits in a protein oligomer. So far none of the allosteric transitions observed in proteins has exceeded the time limit as defined here, indicating a logical consistency between our theory and the experiments.

1. Introduction

Low-frequency motions are vitally important to the function of the human body and human life itself. The blood circulation is driven by the pulsation of the heart, and breathing is carried out by oscillation of the lungs. We walk and eat by oscillating our legs and teeth. Furthermore, we could not even hear and speak without the vibrations of our eardrums and larynges. It is perfectly true that there would be no life and life activities at all if there were no vibration.

Likewise, low-frequency motions also play a significant role in molecular biology although the range of the frequencies is much different from that in macroscopic organs because of the great disparity of the objects in size. During the last decade more and more evidence has emerged indicating that low-frequency modes clearly exist in protein and DNA molecules [1–5]. Many efforts have been made to attempt to reveal the origin of this kind of low-frequency motion [6–13]. Meanwhile, various speculations have been advanced in trying to explore their biological functions from the viewpoint of dynamics, which can be roughly classified as follows:

1. Green [14], Ji [15] and Fröhlich [16] presumed that the catalytic function of an enzyme might be closely related to its internal low-frequency motion.

2. Chou and Chen [17,18] demonstrated that

* Part of this paper was presented at the Department of Biophysics, Kyoto University, Japan and Los Alamos National Laboratory, U.S.A.

** Visiting Professor at Baker Laboratory of Chemistry, Cornell University, from 1983 to 1984.

the associations between insulin and insulin receptor as well as insulin and insulin antibody would concomitantly excite low-frequency phonons (wave numbers: 10–100 cm^{-1}), otherwise a thermodynamic 'deficit' could not be compensated for. Based on this, a physical picture was put forward in which this kind of low-frequency phonon might play a very important role in lowering the threshold value of the allosteric transition and transmitting biological information.

3. Careri et al. [19] and Englander [20] attempted to determine the relationship between the hydrogen exchange properties occurring in proteins and nucleic acids and their internal low-frequency motions.

4. Chou et al. [21] introduced the concept of activating low-frequency phonons, whose excitation and annihilation might be directly associated with the activation and deactivation of a protein molecule, respectively.

5. Zhou [22] and Sobell et al. [23] deduced that the low-frequency (acoustic) phonons might play a vital role in DNA breathing and drug intercalation.

6. Chou [7,10] investigated the influence of the microenvironment concerned upon the low-frequency motion in order to gain an insight into the intrinsic relation between the activity of a protein molecule and its activating low-frequency motion.

7. Chou [12] applied the concept of low-frequency resonance to elucidate the dynamic principles of the cooperative phenomena observed in the reactions between hemoglobins and ligands.

Due to their distinctive physical characters, vibrations in nature play a very prominent role in transmitting various kinds of information. In molecular biology, however, there are plenty of vivid phenomena of information transmission, which are closely relevant to the structures, functions and mechanisms of biomacromolecules. In fact the use of chemical and physical principles to describe and understand the dynamic process of this kind of information transmission has become one of the most important current subjects in molecular biology. To stimulate further the study of this area, it is instructive to address the following question: Will vibrations also play an important role during the transmission of biological information at the molecular level? If so, how? The present study was initiated in an attempt to provide a general discussion concerning the relation between the resonance effect and energy transmission in oligomeric protein molecules.

2. Geometric arrangements of subunits in oligomeric proteins

That large proteins are built up from smaller units noncovalently linked was first discovered by Svedberg and his co-workers [24,25]. However, interest in this kind of quaternary structure of proteins substantially increased only after almost 40 years, when it was realized that broad aspects of cellular control mechanisms and the regulation of enzyme activity might operate at the molecular level through interactions between subunits of an oligomeric protein molecule [26–28].

An extensive study [29] in this field indicated that the majority of oligomeric proteins are composed of two or four subunits. Few proteins have more than 12 subunits. Besides, the majority of protein oligomers have an even number of subunits. Out of 100 proteins listed by Klotz et al. [29], only eight have an odd number of subunits, and these have either three or five.

When protein monomers associate, the number of possible geometric arrangements increases rapidly as the number of subunits increases. However, the number of arrangements can be greatly reduced if the following two restrictions as given by Klotz et al. [29] are imposed: (1) all subunits in an oligomeric protein are in equivalent (or pseudo identical) environments; (2) the bonding potential (or binding regions) of subunits must be saturated. These requirements are reasonable because so far the deductions based on them are in good agreement with observations.

Suppose n is the number of subunits of an oligomeric protein molecule. According to the above two restrictions, there is only one geometric arrangement available for the dimer, trimer or pentamer (i.e., $n = 2$, 3, or 5) as illustrated in fig. 1a, b, or c, respectively. However, for the tetramer (i.e., $n = 4$) we have two possible geometric

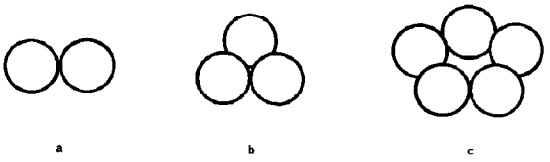

Fig. 1. (a) Dimer: linear arrangement; (b) trimer: triangular arrangement; (c) pentamer: pentagonal arrangement.

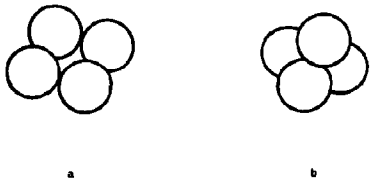

Fig. 2. Tetramer: (a) square arrangement; (b) tetrahedral arrangement.

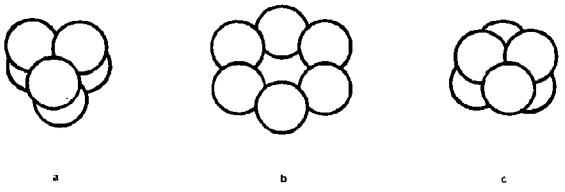

Fig. 3. Hexamer: (a) trigonal prism arrangement; (b) hexagonal arrangement; (c) octahedral arrangement.

arrangements (fig. 2a and b), and for the hexamer three possible arrangements (fig. 3a–c). Following these regulations, we can always determine the possible geometric arrangements for any protein oligomer with a given number of subunits. Actually, the restrictions mentioned above require that the protein oligomer be composed of subunits regularly packed about a central point, and hence the only symmetry possible is that of point groups.

3. Physical picture of low-frequency resonance in a protein oligomer and its general solution

As is well known, a subunit composed of N atoms generally has $3N-6$ vibrational degrees of freedom, and hence corresponds to a spectrum with $3N-6$ vibrational frequencies. However, among these vibrations, only the low-frequency motions possess more significant biological effects. This is because, in the sense of thermodynamics, only the low-frequency vibrations can contribute a larger phonon entropy so as to be able to compensate for the loss of free energy during the association between a protein and its receptor [17,18] that is the first step in transmitting biological information, and, in the sense of dynamics, also only the low-frequency vibrations can generate a greater amplitude, thus facilitating attainment of the considerable intramolecular displacement as required during the allosteric transition of a protein molecule [12]. Furthermore, in the low-frequency spectrum of a native protein molecule, one dominant low-frequency mode [10] usually exists, which corresponds to the maximum low-frequency peak observed in experiments [1,2,4] and can be termed the activating low-frequency mode [7] because it is closely related to the activation and deactivation of a protein molecule [7,21]. Physically speaking, the dominant low-frequency mode represents some kind of internal collective movement in a biological macromolecule and hence involves substantial atoms therein, as described by the continuity model [7,8,10,13,40]. Naturally, this type of motion will play a much more significant role than the others in biological functions such as during the allosteric transition and cooperative effect [12,21] and should therefore be singled out for further study of particular interest. In other words, in order to grasp the essence of the matter, our attention should be focused upon the dominant low-frequency mode rather than the whole frequency spectrum of a protein molecule. This not only can greatly simplify our mathematical treatment, but also makes the physical picture very clear.

Now suppose such a dominant low-frequency mode in each subunit of a protein oligomer is characterized in terms of an effective mass m and an inherent force constant k^0. Note that m and k^0 are just two physical quantities used to describe phenomenologically the dominant low-frequency motion of a subunit. Furthermore, according to the analysis in section 2, the noncovalent linkage (or bonding potential) between the i-th and the j-th subunits can be compared to a coupling spring whose force constant is assumed to be k_{ij}^*. Thus, a physical picture of a vibration-coupled system for a protein oligomer emerges naturally, and can be

formulated as follows:

The kinetic energy T and potential energy U of such a vibration-coupled system are given by:

$$\begin{cases} T = \dfrac{m}{2}\sum_{i=1}^{n}\dot{q}_i^2 & (1) \\ U = \dfrac{k^0}{2}\sum_{i=1}^{n} q_i^2 + \frac{1}{2}\sum_{i\neq j} k_{ij}(q_i + q_j)^2 & (2) \end{cases}$$

where q_i is the dominant low-frequency vibrational coordinate of the ith subunit, n the number of the total subunits in a protein oligomer, and k_{ij} is related to k_{ij}^* and the geometric arrangement of the subunits, as will be explicitly given for the concrete examples discussed later. Thus, according to the Lagrange equation

$$\frac{\mathrm{d}}{\mathrm{d}t}\left(\frac{\partial L}{\partial \dot{q}_i}\right) - \frac{\partial L}{\partial q_i} = 0 \qquad (3)$$

$$L = T - U \quad (i = 1, 2, \ldots, n)$$

we have

$$-\ddot{q}_i = \sum_{j=1}^{n} a_{ij} q_j \qquad (4)$$

$$(i = 1, 2, \ldots, n)$$

where

$$a_{ij} = \begin{cases} \dfrac{k^0 + \sum_{j=1}^{n} k_{ij}}{m} & \text{if } i = j \\ \dfrac{k_{ij}}{m} & \text{if } i \neq j \end{cases} \qquad (5)$$

in which, by definition, $k_{ij} = 0$ if $i = j$, and $k_{ij} = k_{ji}$. Besides, for most protein oligomers, the following circulant condition also holds [29]

$$\left.\begin{aligned} k_{ij} &= k_{(i+1)(j+1)} \\ k_{i(j+n)} &= k_{(i+n)j} = k_{ij} \end{aligned}\right\} \qquad (6)$$

Thus, the vibrational coordinate of the i-th subunit (hereafter, the term vibration always denotes the dominant low-frequency vibration) can be expressed as (see appendix for derivation):

$$q_i = \sum_{l=1}^{n} c_{il} A_l \cos(\omega_l t + \phi_l) \qquad (7)$$

$$(i = 1, 2, \ldots, n)$$

where

$$\omega_l^2 = b_1 + 2b_2\cos(2l\pi/n) + 2b_3\cos(4l\pi/n) + \ldots + \begin{cases} b_{(n/2)+1}\cos(l\pi) \\ \quad \text{if } n \text{ is an even number} \\ 2b_{(n+1)/2}\cos[l(n-1)\pi/n] \\ \quad \text{if } n \text{ is an odd number} \end{cases} \qquad (8)$$

$$(l = 1, 2, \ldots, n)$$

in which

$$b_q = \begin{cases} \dfrac{k^0 + \sum_{j=1}^{n} k_{1j}}{m} & \text{if } q = 1 \\ \dfrac{k_{1q}}{m} & \text{if } q \neq 1 \end{cases} \qquad (9)$$

and

$$\begin{bmatrix} C_{1l} \\ C_{2l} \\ C_{3l} \\ \vdots \\ C_{nl} \end{bmatrix} = \begin{bmatrix} C_1 \\ C_2 \\ C_3 \\ \vdots \\ C_n \end{bmatrix}_l$$

$$= \begin{cases} \begin{bmatrix} 1 \\ \cos(2l\pi/n) \\ \cos(4l\pi/n) \\ \vdots \\ \cos[2(n-1)l\pi/n] \end{bmatrix} \\ \quad \text{for } l = \begin{cases} 1, 2, \ldots, n/2 \text{ for even } n \\ 1, 2, \ldots, (n-1)/2 \text{ for odd } n \end{cases} \\ \begin{bmatrix} 0 \\ -\sin(2l\pi/n) \\ -\sin(4l\pi/n) \\ \vdots \\ -\sin[2(n-1)l\pi/n] \end{bmatrix} \\ \quad \text{for } l = \begin{cases} (n+2)/2, \ldots, (n-1) \text{ for even } n \\ (n+1)/2, \ldots, (n-1) \text{ for odd } n \end{cases} \\ \begin{bmatrix} 1 \\ 1 \\ 1 \\ \vdots \\ 1 \end{bmatrix} \quad \text{for } l = n \end{cases} \qquad (10)$$

In eq. 7, A_l ($l = 1, 2, \ldots, n$) are the constants to be determined according to the initial condition of a vibration-coupled system.

Eqs. 7–10 are the general solutions for a protein oligomer as described by a dominant low-frequency resonance-coupled system.

4. Energy transmission and cooperative phenomena

In this section, we shall use the general solutions obtained in section 3 to discuss some concrete protein oligomers.

Before proceeding, some points should be addressed so as to make the results obtained below have more clear biological implications. As is well known, for a given dominant low-frequency mode, the larger the amplitude is, the more the corresponding phonons will be excited [7,10] and the greater the relevant subunit will be in energy. Therefore, the following two aspects are naturally reflected by the amplitude, and are both closely related to biological function. (1) The aspect of the conformation. When the dominant low-frequency amplitude of a subunit reaches its maximum value, the subunit can be thought of as more easily reaching (or as being triggered to become) the 'relaxed state' according to Perutz [30], or the 'activated state' according to Chou et al. [21] and Chou [12]; when the amplitude is at a minimum, however, a conformational change in that subunit is hardly triggered, and hence it is quite stable in the 'tense state' [30] or the 'inactivated state' [12]. A subunit in the former state has a greater probability of binding a ligand, but the probability of a subunit in the latter binding a ligand is much smaller relatively [21] and is negligible in comparison with the former. (2) The aspect of energetics. When the dominant low-frequency amplitude of a subunit is larger, its active site will more easily be able to attain a high activation energy level, or overcome the barrier of activation energy, so as to decrease the 'threshold value' [17] required for a successful reaction and thus facilitate ligand binding. Consequently, the variation in the dominant low-frequency amplitudes among various subunits in a protein oligomer will reflect not only the physically coupled effects among those subunits but also their mutual influence in biological function.

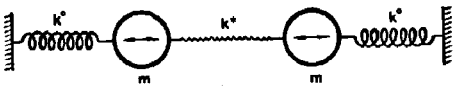

Fig. 4. Schematic representation of the vibration-coupled system of a protein dimer. The arrow represents the vibrational direction of the dominant low-frequency mode in each subunit.

Here let us first define the following quantities that are commonly used for all the examples considered in this section:

$$\omega_0^2 = k^0/m = 2\pi c\tilde{\nu}_0, \; x = k^*/k^0 \tag{11}$$

where k^0 and m are the inherent force constant and effective mass of each subunit, characterizing its dominant low-frequency motion (see figs. 4, 6, 8 and 12), c the speed of light in a vacuum, k^* the force constant of an equivalent spring linking any two neighbor subunits, and ω_0 and $\tilde{\nu}_0$ the corresponding circular frequency and wave number of the dominant low-frequency mode, respectively. As will be illustrated in the following examples, the k_{ij} in eq. 2 will be determined by k^* as well as the concrete geometric arrangement of the subunits in a protein oligomer.

4.1. Protein dimer (fig. 1a)

The vibration-coupled system for a protein dimer is visualized as in fig. 4. In the present case, we obviously have $k_{12} = k^*$, and hence (cf. eq. 9):

$$n = 2, \; b_1 = (k^0 + k^*)/m, \; b_2 = k^*/m \tag{12}$$

Substituting eq. 12 into eqs. 8 and 10, we obtain

$$\omega_1^2 = k^0/m, \; \omega_2^2 = (k^0 + 2k^*)/m \tag{13}$$

$$\begin{bmatrix} C_1 \\ C_2 \end{bmatrix}_1 = \begin{bmatrix} 1 \\ -1 \end{bmatrix}, \begin{bmatrix} C_1 \\ C_2 \end{bmatrix}_2 = \begin{bmatrix} 1 \\ 1 \end{bmatrix} \tag{14}$$

Therefore, the general solution for q_i (cf. eq. 7) is

$$q_1 = A_1 \cos(\omega_1 t + \phi_1) + A_2 \cos(\omega_2 t + \phi_2)$$

$$q_2 = -A_1 \cos(\omega_1 t + \phi_1) + A_2 \cos(\omega_2 t + \phi_2)$$

Suppose at $t = 0$, $q_1 = A$, $q_2 = \dot{q}_1 = \dot{q}_2 = 0$, the coefficients in the above equations can thus be determined as $A_1 = A/2$, $A_2 = A/2$, $\phi_1 = \phi_2 = 0$; i.e.

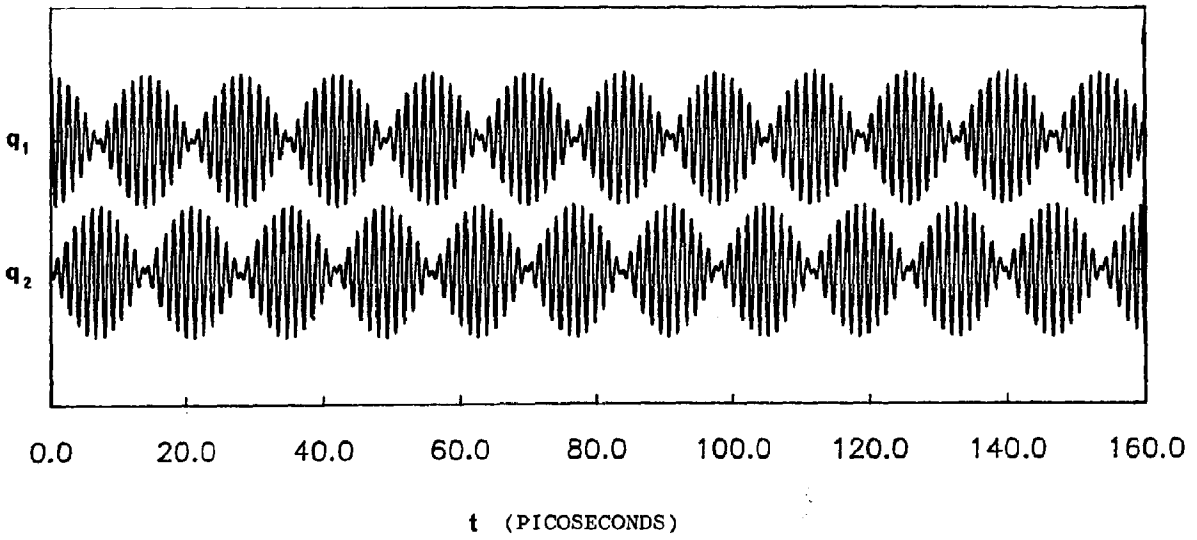

Fig. 5. Plot of q_1 and q_2 vs. t (see eq. 15) when $x = 0.1$, $\omega_0 = 4.71 \times 10^{12}$/s (i.e., $\bar{\nu}_0 = 25\ \mathrm{cm}^{-1}$).

$$\left.\begin{aligned} q_1 &= \frac{A}{2}\cos\left(\sqrt{k^0/m}\ t\right) + \frac{A}{2}\cos\left(\sqrt{(k^0+2k^*)/m}\ t\right) \\ &= \frac{A}{2}\cos\omega_0 t + \frac{A}{2}\cos\left(\sqrt{1+2x}\,\omega_0 t\right) \\ q_2 &= -\frac{A}{2}\cos\left(\sqrt{k^0/m}\ t\right) \\ &\quad + \frac{A}{2}\cos\left(\sqrt{(k^0+2k^*)/m}\ t\right) \\ &= -\frac{A}{2}\cos\omega_0 t + \frac{A}{2}\cos\left(\sqrt{1+2x}\,\omega_0 t\right) \end{aligned}\right\} \quad (15)$$

For real systems, we generally have $x \ll 1$. When $x = 0.1$ and $\nu_0 = 25\ \mathrm{cm}^{-1}$ [4], i.e., $\omega_0 = 4.71 \times 10^{12}$/s, from the plot of q_1 and q_2 vs. t given in fig. 5, it can be seen that when the amplitude of the second subunit reaches the maximum, that of the first subunit becomes minimum, and vice versa. Such a conclusion can also be obtained in the following way. When $x \ll 1$, to the first-order approximation of x, eq. 15 can be written as

$$\left.\begin{aligned} q_1 &\simeq Q_1 \cos[(1 + x/2)\omega_0 t] \\ q_2 &\simeq Q_2 \sin[(1 + x/2)\omega_0 t] \end{aligned}\right\} \quad (16)$$

where

$$Q_1 = A\cos(x\omega_0 t/2),\ Q_2 = -A\sin(x\omega_0 t/2) \quad (17)$$

which clearly indicates the alternate character of variation of the two amplitudes. From the point of view of energetics, the above result indicates that the vibrational energy will flow cyclically from one subunit to the other. If there is no damping effect, such a phenomenon will go on forever. Even when a damping effect exists, however, the fundamental physical picture of energy transmission through the resonance mechanism would still remain approximately the same except in intensity, as will be further discussed later. This feature was once applied by Luisi and Zandomeneghi [31] to interpret the phenomenon of the half-of-the-sites reactivity of oligomeric enzymes [32,33]. However, it seems much more interesting to apply this result to elucidate the dynamic process of cooperativity in an oligomeric protein, as follows.

As mentioned at the beginning of this section, the larger the dominant low-frequency amplitude in a subunit is, the easier will be its active site in binding a ligand, implying that the activation energy required for binding with a ligand is lower. The dominant low-frequency amplitude of a subunit due to Brownian thermal collision is very small [7,8,12], so the activation energy for combining with a ligand at the beginning is relatively much larger. However, as soon as one subunit binds to a ligand, as a consequence of release of

energy from the occupied site due to the binding reaction, the low-frequency amplitude of this subunit will be first driven to experience a sudden and drastic increment, and then the energy will be transmitted to the other subunit via the resonance-coupled mechanism, leading to a drastic increase in amplitude as well for the second subunit and triggering a conformational change at its active site so as to make its binding with a ligand much more favorable, as observed in cooperative reactions. What is particularly interesting is that, if the cooperativity is controlled by such a process of energy transmission, we will be able to define the lower time limit of an allosteric transition, one of the most fundamental limit scales in biomolecular dynamics, by the following approach. Define

$$T^{i\to j} \equiv \text{the shortest time-interval from } \max|q_i| \text{ to } \max|q_j| \quad (18)$$

thus, for the present example, we have (cf. eq. 17):

$$T^{1\to 2} = \pi/(x\omega_0) = 1/(2xc\tilde{\nu}_0) \quad (19)$$

For insulin dimer, $\tilde{\nu}_0 = 22\ \text{cm}^{-1}$ [4,8], we obtain $T^{1\to 2} \simeq 7\times 10^{-12}$ s if $x = 0.1$.

The above concept implies that the speed of an allosteric transition cannot exceed that of the energy flow via a resonance-coupled mechanism. In other words, the allosteric transition is 'resonance-controlled', in contrast to the concept of a 'diffusion-controlled reaction' in enzyme kinetics [34–36]. Further discussion on such an idea will be given later.

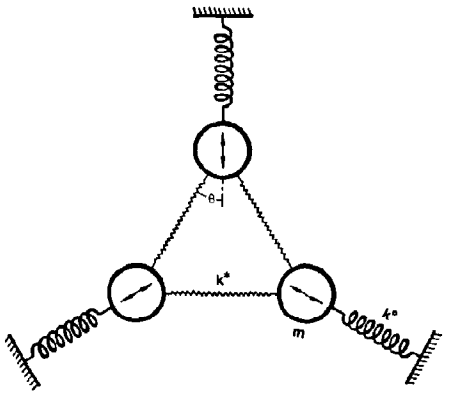

Fig. 6. Schematic representation of the vibration-coupled system of a protein trimer. The arrows have the same implication as in fig. 4.

4.2. Protein trimer (fig. 1b)

The corresponding vibration coupled scheme is given in fig. 6, from which we have $k_{12} = k_{13} = k_{23} = k^* \cos^2\theta$ and hence (cf. eq. 9):

$$\left.\begin{aligned} &n = 3,\ \theta = 30°, \\ &b_1 = \frac{k^0 + 2k^*(\cos\theta)^2}{m} = (1 + 3x/2)\,\omega_0^2 \\ &b_2 = b_3 = k^*(\cos\theta)^2/m = 3x\omega_0^2/4 \end{aligned}\right\} \quad (20)$$

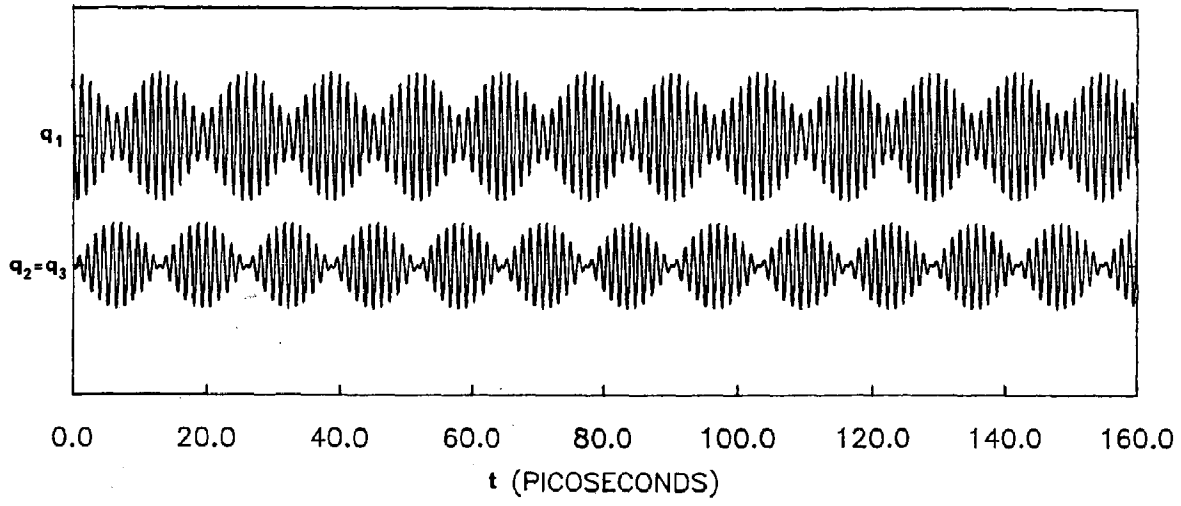

Fig. 7. Plot of q_1 and $q_2 = q_3$ vs. t (see eq. 23) when $x = 0.1$, $\omega_0 = 4.71\times 10^{12}$/s (i.e. $\tilde{\nu}_0 = 25\ \text{cm}^{-1}$).

Substituting eq. 20 into eqs. 8 and 10, we obtain

$$\left.\begin{aligned}\omega_1^2 = \omega_2^2 &= \frac{k^0 + 3k^*/4}{m} = (1 + 3x/4)\omega_0^2 \\ \omega_3^2 &= (k^0 + 3k^*)/m = (1 + 3x)\omega_0^2\end{aligned}\right\} \tag{21}$$

$$\begin{bmatrix} C_1 \\ C_2 \\ C_3 \end{bmatrix}_1 = \begin{bmatrix} 1 \\ -1/2 \\ -1/2 \end{bmatrix}, \quad \begin{bmatrix} C_1 \\ C_2 \\ C_3 \end{bmatrix}_2 = \begin{bmatrix} 0 \\ \sqrt{3}/2 \\ -\sqrt{3}/2 \end{bmatrix},$$

$$\begin{bmatrix} C_1 \\ C_2 \\ C_3 \end{bmatrix}_3 = \begin{bmatrix} 1 \\ 1 \\ 1 \end{bmatrix} \tag{22}$$

Suppose at $t = 0$, $q_1 = A$, $q_2 = q_3 = \dot{q}_1 = \dot{q}_2 = \dot{q}_3 = 0$, following the same procedures as in the last example, we obtain

$$\left\{\begin{aligned} q_1 &= \frac{2A}{3}\cos\left(\sqrt{1 + 3x/4}\,\omega_0 t\right) + \frac{A}{3}\cos\left(\sqrt{1 + 3x}\,\omega_0 t\right) \\ q_2 = q_3 &= -\frac{A}{3}\cos\left(\sqrt{1 + 3x/4}\,\omega_0 t\right) + \frac{A}{3}\cos\left(\sqrt{1 + 3x}\,\omega_0 t\right) \end{aligned}\right. \tag{23}$$

The plot of q_1, $q_2 = q_3$ vs. t is given in fig. 7, from which we see that when the amplitude of the first subunit becomes minimum, the amplitudes of the second and third subunits reach the maximum, and vice versa. This demonstrates that the vibration energy is transmitted to the second and third subunits equally and synchronously from the first subunit. Likewise, when $x \ll 1$, eq. 23 can be expressed as

$$\left\{\begin{aligned} q_1 &\simeq \frac{A}{3}\cos\left[\left(1 + \frac{3x}{8}\right)\omega_0 t\right] + \frac{2A}{3}\cos\left[\left(1 + \frac{15x}{16}\right)\omega_0 t\right]\cos(9x\omega_0 t/16) \\ q_2 = q_3 &\simeq -\frac{2A}{3}\sin\left[\left(1 + \frac{15x}{16}\right)\omega_0 t\right] \times \sin(9x\omega_0 t/16) \end{aligned}\right. \tag{24}$$

From the above it can be seen that the maximum amplitudes of the second and third subunits are $2A/3$, while the minimum amplitude of the first subunit is $A/3$. Therefore, we have $(2A/3)^2 + (2A/3)^2 + (A/3)^2 = A^2$, just reflecting the relation of energy conservation because, as is well known, the vibration energy $E_i \sim |q_i|^2$. From eq. 24 we can also find (cf. eq. 18):

$$T^{1\to 2} = T^{1\to 3} = 8\pi/9x\omega_0 = 4/9xc\tilde{\nu}_0 = 5.92 \text{ ps} \tag{25}$$

4.3. Protein tetramer

4.3.1. *Square arrangement* (fig. 2a)

The corresponding vibration-coupled system is illustrated in fig. 8, from which with eq. 2 we have $k_{12} = k_{14} = k^* \cos^2\theta$, $k_{13} = 0$, and hence (cf. eq. 9):

$$\left\{\begin{aligned} n = 4,\ \theta = 45°,\ b_1 &= \frac{k^0 + 2k^*(\cos\theta)^2}{m} \\ &= (1 + x)\omega_0^2 \\ b_2 = b_4 &= k^*(\cos\theta)^2/m = x\omega_0^2/2,\ b_3 = 0 \end{aligned}\right. \tag{26}$$

Substitution of eq. 26 into eqs. 8 and 10 will give

$$\left\{\begin{aligned} \omega_1^2 = \omega_3^2 &= (k^0 + k^*)/m \\ &= (1 + x)\omega_0^2 \text{ (double degeneracy)} \\ \omega_2^2 &= k^0/m = \omega_0^2, \\ \omega_4^2 &= (k^0 + 2k^*)/m = (1 + 2x)\omega_0^2 \end{aligned}\right. \tag{27}$$

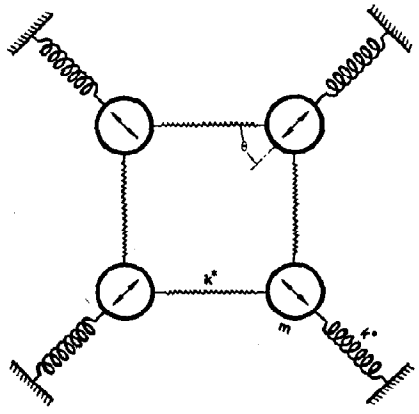

Fig. 8. Schematic representation of the vibration-coupled system of a protein tetramer with square arrangement. The implication of the arrows is the same as in fig. 4.

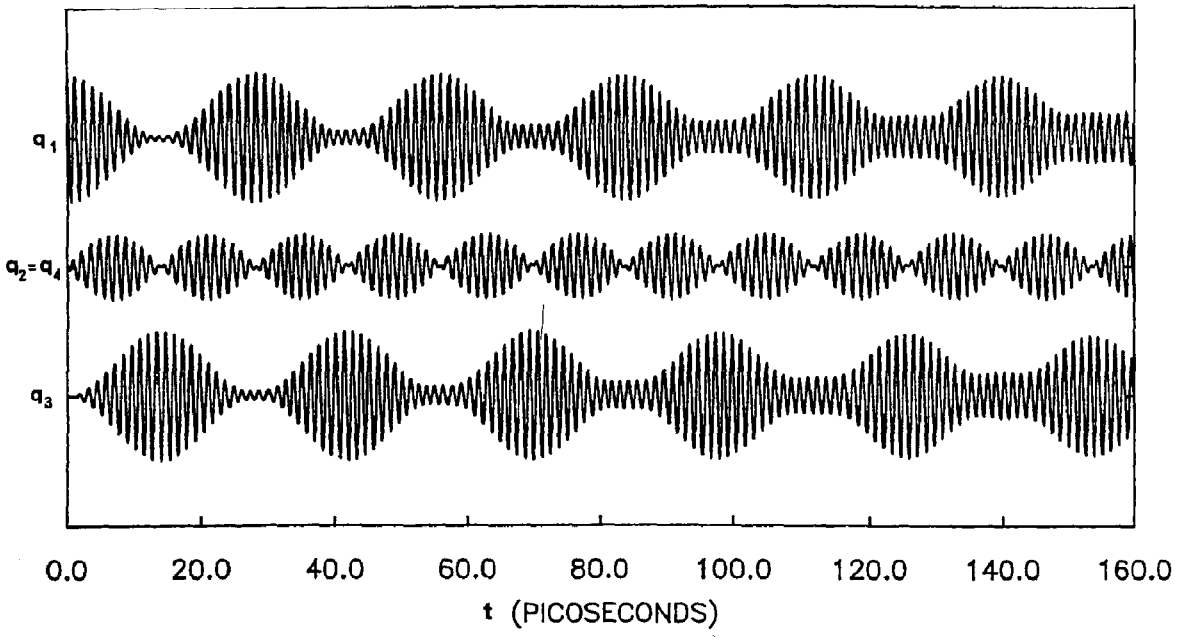

Fig. 9. Plot of q_1, $q_2 = q_4$ and q_3 vs. t (see eq. 29) when $x = 0.1$ and $\omega_0 = 4.71 \times 10^{12}$/s (i.e., $\nu_0 = 25$ cm^{-1}).

$$\begin{bmatrix} C_1 \\ C_2 \\ C_3 \\ C_4 \end{bmatrix}_1 = \begin{bmatrix} 1 \\ 0 \\ -1 \\ 0 \end{bmatrix}, \begin{bmatrix} C_1 \\ C_2 \\ C_3 \\ C_4 \end{bmatrix}_2 = \begin{bmatrix} 1 \\ -1 \\ 1 \\ -1 \end{bmatrix},$$

$$\begin{bmatrix} C_1 \\ C_2 \\ C_3 \\ C_4 \end{bmatrix}_3 = \begin{bmatrix} 0 \\ 1 \\ 0 \\ -1 \end{bmatrix}, = \begin{bmatrix} C_1 \\ C_2 \\ C_3 \\ C_4 \end{bmatrix}_4 = \begin{bmatrix} 1 \\ 1 \\ 1 \\ 1 \end{bmatrix} \tag{28}$$

Thus, if $q_1 = A$, $q_2 = q_3 = q_4 = \dot{q}_1 = \dot{q}_2 = \dot{q}_3 = \dot{q}_4 = 0$ at $t = 0$, we obtain

$$\begin{cases} q_1 = \dfrac{A}{2}\cos\left(\sqrt{1+x}\,\omega_0 t\right) + \dfrac{A}{4}\cos\omega_0 t \\ \qquad + \dfrac{A}{4}\cos\left(\sqrt{1+2x}\,\omega_0 t\right) \\ q_2 = q_4 = -\dfrac{A}{4}\cos\omega_0 t + \dfrac{A}{4}\cos\left(\sqrt{1+2x}\,\omega_0 t\right) \\ q_3 = -\dfrac{A}{2}\cos\left(\sqrt{1+x}\,\omega_0 t\right) + \dfrac{A}{4}\cos\omega_0 t \\ \qquad + \dfrac{A}{4}\cos\left(\sqrt{1+2x}\,\omega_0 t\right) \end{cases} \tag{29}$$

When $x = 0.1$ and $\omega_0 = 4.71 \times 10^{12}$ s (i.e., $\tilde{\nu}_0 = 25$ cm^{-1}), it can be seen from the plot of q vs. t given in fig. 9, that, for the square protein oligomer, the energy excited in the first subunit can be transmitted only partly to the second and fourth (adjacent) subunits, but can be transmitted almost completely to the third (diagonal) subunit. Consequently, for this kind of quaternary structure, the energy transmitted from a subunit to its diagonal subunit is more favorable than to its adjacent subunit; the former is almost 4-times the size of the latter. Based on such a conclusion, it can be predicted that, after a subunit is bound to a ligand, the next subunit to bind with a ligand is more likely the diagonal one since its induced activation [21] is much more efficient and thorough, so that less binding activation energy is required in comparison with the two adjacent subunits. It can also be seen from fig. 9 that, with increasing time, $\max|q_1|$ and $\max|q_3|$ decrease slightly, but $\min|q_1|$ and $\min|q_3|$ have just the opposite variation, increasing gradually. This is a phenomenon of dispersion due to the contribution of the higher-order terms of x. In fact, when expanding eq. 29, if only the zeroth-order and first-order terms of x are

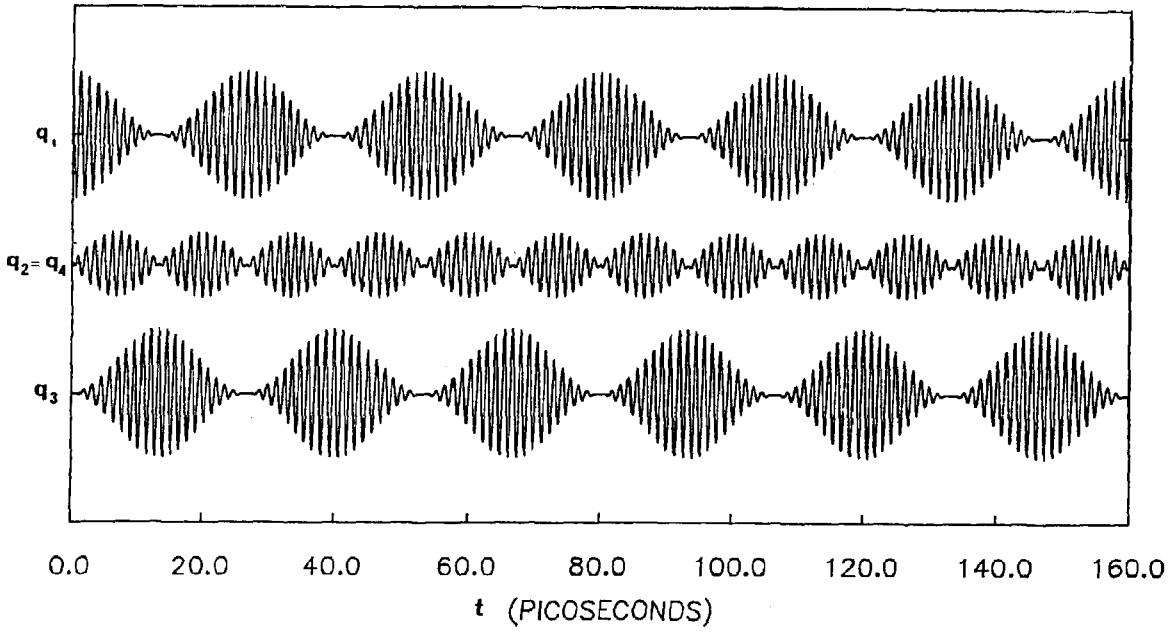

Fig. 10. Plot of q_1, $q_2 = q_4$ and q_3 vs. t when $x = 0.1$, $\omega_0 = 4.71 \times 10^{12}$/s (i.e., $\tilde{\nu}_0 = 25\ \mathrm{cm}^{-1}$) and all contributions from those higher than the first-order term of x are neglected as reflected in eq. 30.

retained, it follows

$$\begin{cases} q_1 \simeq \dfrac{A}{2}\left[1 + \cos(x\omega_0 t/2)\right] \cos\left[(1 + x/2)\omega_0 t\right] \\ q_2 = q_4 \simeq -\dfrac{A}{2} \sin(x\omega_0 t/2) \sin\left[(1 + x/2)\omega_0 t\right] \\ q_3 \simeq \dfrac{A}{2}\left[\cos(x\omega_0 t/2) - 1\right] \cos\left[(1 + x/2)\omega_0 t\right] \end{cases} \tag{30}$$

A plot of q_i ($i = 1$–4) vs. t in this case is given in fig. 10, in which no dispersion occurs at all. From eq. 42 we can also easily find (cf. eq. 18)

$$\begin{cases} T^{1\to 2} = T^{1\to 4} = \pi/x\omega_0 = 1/2xc\tilde{\nu}_0 = 6.67\ \text{ps} \\ T^{1\to 3} = 2\pi/x\omega_0 = 1/xc\tilde{\nu}_0 = 13.34\ \text{ps} \end{cases} \tag{31}$$

when $x = 0.1$. Note $T^{1\to 3}$ is two times of $T^{1\to 2}$ and $T^{1\to 3}$.

4.3.2. Tetrahedron arrangement (fig. 2b)

In this case we should instead have $k_{12} = k_{13} = k_{14} = k^* \cos^2\theta$, and thus (cf. eq. 9):

$$\begin{cases} n = 4,\ \theta = \cos^{-1}(\sqrt{6}/3) \simeq 35.26^\circ \\ b_1 = \left[k^0 + 3k^*(\cos\theta)^2\right]/m = (1 + 2x)\omega_0^2 \\ b_2 = b_3 = b_4 = k^*(\cos\theta)^2/m = 2x\omega_0^2/3 \end{cases} \tag{32}$$

Therefore, the corresponding eigenvalues and eigenvectors become

$$\begin{cases} \omega_1^2 = \omega_2^2 = \omega_3^2 = (k^0 + 4k^*/3)/m \\ \quad = (1 + 4x/3)\omega_0^2 \text{ (triple degeneracy)} \\ \omega_4^2 = (k^0 + 4k^*)/m = (1 + 4x)\omega_0^2 \end{cases} \tag{33}$$

$$\begin{bmatrix} C_1 \\ C_2 \\ C_3 \\ C_4 \end{bmatrix}_1 = \begin{bmatrix} 1 \\ 0 \\ -1 \\ 0 \end{bmatrix}, \begin{bmatrix} C_1 \\ C_2 \\ C_3 \\ C_4 \end{bmatrix}_2 = \begin{bmatrix} 1 \\ -1 \\ 1 \\ -1 \end{bmatrix},$$

$$\begin{bmatrix} C_1 \\ C_2 \\ C_3 \\ C_4 \end{bmatrix}_3 = \begin{bmatrix} 0 \\ 1 \\ 0 \\ -1 \end{bmatrix}, \begin{bmatrix} C_1 \\ C_2 \\ C_3 \\ C_4 \end{bmatrix}_4 = \begin{bmatrix} 1 \\ 1 \\ 1 \\ 1 \end{bmatrix} \tag{34}$$

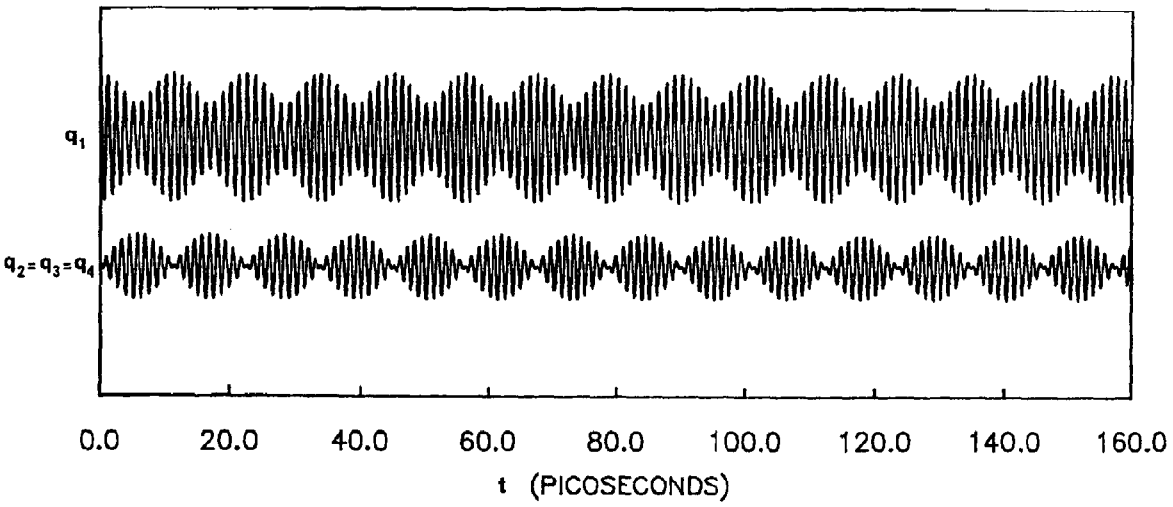

Fig. 11. Plot of q_1 and $q_2 = q_3 = q_4$ vs. t when $x = 0.1$ and $\omega_0 = 4.71 \times 10^{12}$/s (i.e., $\tilde{\nu}_0 = 25\ \mathrm{cm}^{-1}$).

The same initial condition as in the last example (square arrangement) will now give

$$\begin{cases} q_1 = \dfrac{3A}{4}\cos\left(\sqrt{1+4x/3}\,\omega_0 t\right) \\ \qquad + \dfrac{A}{4}\cos\left(\sqrt{1+4x}\,\omega_0 t\right) \\ q_2 = q_3 = q_4 = -\dfrac{A}{4}\cos\left(\sqrt{1+4x/3}\,\omega_0 t\right) \\ \qquad + \dfrac{A}{4}\cos\left(\sqrt{1+4x}\,\omega_0 t\right) \end{cases} \tag{35}$$

whose plot with respect to t is given in fig. 11. Therefore, for the tetrahedron protein oligomer, the energy excited in the first subunit will be transmitted to the other three subunits equally and synchronously as shown in fig. 11, which is much different from the case in the square protein oligomer (see fig. 9). Likewise, we have

$$\begin{cases} q_1 \simeq \dfrac{A}{2}\cos\left[(1+2x/3)\omega_0 t\right] + \dfrac{A}{2}\cos(2x\omega_0 t/3) \\ \qquad \times \cos\left[(1+4x/3)\omega_0 t\right] \\ q_2 = q_3 = q_4 = -\dfrac{A}{2}\sin(2x\omega_0 t/3) \\ \qquad \times \sin\left[(1+4x/3)\omega_0 t\right] \end{cases} \tag{36}$$

from which we obtain

$$T^{1\to 2} = T^{1\to 3} = T^{1\to 4} = 3\pi/4x\omega_0 = 3/8xc\tilde{\nu}_0 = 5.00\ \mathrm{ps} \tag{37}$$

4.4. Protein hexamer with hexagon arrangement (fig. 3b)

The corresponding vibration-coupled system is illustrated in fig. 12, from which with eq. 2 we have $k_{12} = k_{16} = k^* \cos^2\theta$, $k_{13} = k_{14} = k_{15} = 0$, and hence (cf. eq. 9):

$$\begin{cases} n = 6,\ \theta = 60^\circ \\ b_1 = \left[k^0 + 2k^*(\cos\theta)^2\right]/m = (1+x/2)\omega_0^2 \\ b_2 = b_6 = k^*(\cos\theta)^2/m = x\omega_0^2/4 \\ b_3 = b_4 = b_5 = 0 \end{cases} \tag{38}$$

Substituting eq. 38 into eqs. 8 and 10, we obtain

$$\begin{cases} \omega_1^2 = \omega_5^2 = (k^0 + 3k^*/4)m = (1+3x/4)\omega_0^2 \\ \quad \text{(double degeneracy)} \\ \omega_2^2 = \omega_4^2 = (k^0 + k^*/4)/m = (1+x/4)\omega_0^2 \\ \quad \text{(double degeneracy)} \\ \omega_3^2 = k^0/m = \omega_0^2,\ \omega_6^2 = (k^0 + k^*)/m = (1+x). \end{cases} \tag{39}$$

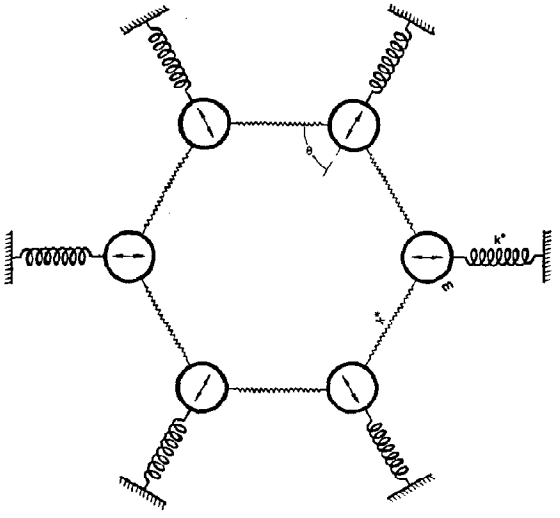

Fig. 12. Schematic representation of the vibration-coupled system of a protein hexamer with hexagonal arrangement. The arrows have the same implication as in fig. 4.

$$\begin{bmatrix} C_1 \\ C_2 \\ C_3 \\ C_4 \\ C_5 \\ C_6 \end{bmatrix}_1 = \begin{bmatrix} 1 \\ 1/2 \\ -1/2 \\ -1 \\ -1/2 \\ 1/2 \end{bmatrix}, \quad \begin{bmatrix} C_1 \\ C_2 \\ C_3 \\ C_4 \\ C_5 \\ C_6 \end{bmatrix}_2 = \begin{bmatrix} 1 \\ -1/2 \\ -1/2 \\ 1 \\ -1/2 \\ -1/2 \end{bmatrix},$$

$$\begin{bmatrix} C_1 \\ C_2 \\ C_3 \\ C_4 \\ C_5 \\ C_6 \end{bmatrix}_3 = \begin{bmatrix} 1 \\ -1 \\ 1 \\ -1 \\ 1 \\ -1 \end{bmatrix}, \quad \begin{bmatrix} C_1 \\ C_2 \\ C_3 \\ C_4 \\ C_5 \\ C_6 \end{bmatrix}_4 = \begin{bmatrix} 0 \\ \sqrt{3}/2 \\ -\sqrt{3}/2 \\ 0 \\ \sqrt{3}/2 \\ -\sqrt{3}/2 \end{bmatrix},$$

$$\begin{bmatrix} C_1 \\ C_2 \\ C_3 \\ C_4 \\ C_5 \\ C_6 \end{bmatrix}_5 = \begin{bmatrix} 0 \\ \sqrt{3}/2 \\ \sqrt{3}/2 \\ 0 \\ -\sqrt{3}/2 \\ -\sqrt{3}/2 \end{bmatrix}, \quad \begin{bmatrix} C_1 \\ C_2 \\ C_3 \\ C_4 \\ C_5 \\ C_6 \end{bmatrix}_6 = \begin{bmatrix} 1 \\ 1 \\ 1 \\ 1 \\ 1 \\ 1 \end{bmatrix} \tag{40}$$

Suppose at $t = 0$, $q_1 = A$, $q_2 = q_3 = q_4 = q_5 = q_6 = \dot{q}_1 = \dot{q}_2 = \dot{q}_3 = \dot{q}_4 = \dot{q}_5 = \dot{q}_6 = 0$, following the same procedures as before, we finally obtain

$$q_1 = \frac{A}{3}\cos\left(\sqrt{1 + 3x/4}\,\omega_0 t\right) + \frac{A}{3}\cos\left(\sqrt{1 + x/4}\,\omega_0 t\right) + \frac{A}{6}\cos\omega_0 t + \frac{A}{6}\cos\left(\sqrt{1 + x}\,\omega_0 t\right) \tag{41a}$$

$$q_2 = q_6 = \frac{A}{6}\cos\left(\sqrt{1 + 3x/4}\,\omega_0 t\right) - \frac{A}{6}\cos\left(\sqrt{1 + x/4}\,\omega_0 t\right) - \frac{A}{6}\cos\omega_0 t + \frac{A}{6}\cos\left(\sqrt{1 + x}\,\omega_0 t\right) \tag{41b}$$

$$q_3 = q_5 = \frac{-A}{6}\cos\left(\sqrt{1 + 3x/4}\,\omega_0 t\right) - \frac{A}{6}\cos\left(\sqrt{1 + x/4}\,\omega_0 t\right) + \frac{A}{6}\cos\omega_0 t + \frac{A}{6}\cos\left(\sqrt{1 + x}\,\omega_0 t\right) \tag{41c}$$

$$q_4 = -\frac{A}{3}\cos\left(\sqrt{1 + 3x/4}\,\omega_0 t\right) + \frac{A}{3}\cos\left(\sqrt{1 + x/4}\,\omega_0 t\right) - \frac{A}{6}\cos\omega_0 t + \frac{A}{6}\cos\left(\sqrt{1 + x}\,\omega_0 t\right) \tag{41d}$$

The plot of q_1, q_2, q_3, q_4, q_5, q_6 vs. t is given in fig. 13. Likewise, it would help our further discussion if eq. 41 is expressed in the first-order approximation of x, as follows:

$$\begin{cases} q_1 \simeq Q_1 \cos[(1 + x/4)\omega_0 t] \\ q_2 = q_6 \simeq Q_2 \sin[(1 + x/4)\omega_0 t] \\ q_3 = q_5 \simeq Q_3 \cos[(1 + x/4)\omega_0 t] \\ q_4 \simeq Q_4 \sin[(1 + x/4)\omega_0 t] \end{cases} \tag{42}$$

where

$$\begin{cases} Q_1 = \frac{A}{3}[2\cos(x\omega_0 t/8) + \cos(x\omega_0 t/4)] \\ Q_2 = \frac{-A}{3}[\sin(x\omega_0 t/8) + \sin(x\omega_0 t/4)] \\ Q_3 = \frac{-A}{3}[\cos(x\omega_0 t/8) - \cos(x\omega_0 t/4)] \\ Q_4 = \frac{A}{3}[2\sin(x\omega_0 t/8) - \sin(x\omega_0 t/4)] \end{cases} \tag{43}$$

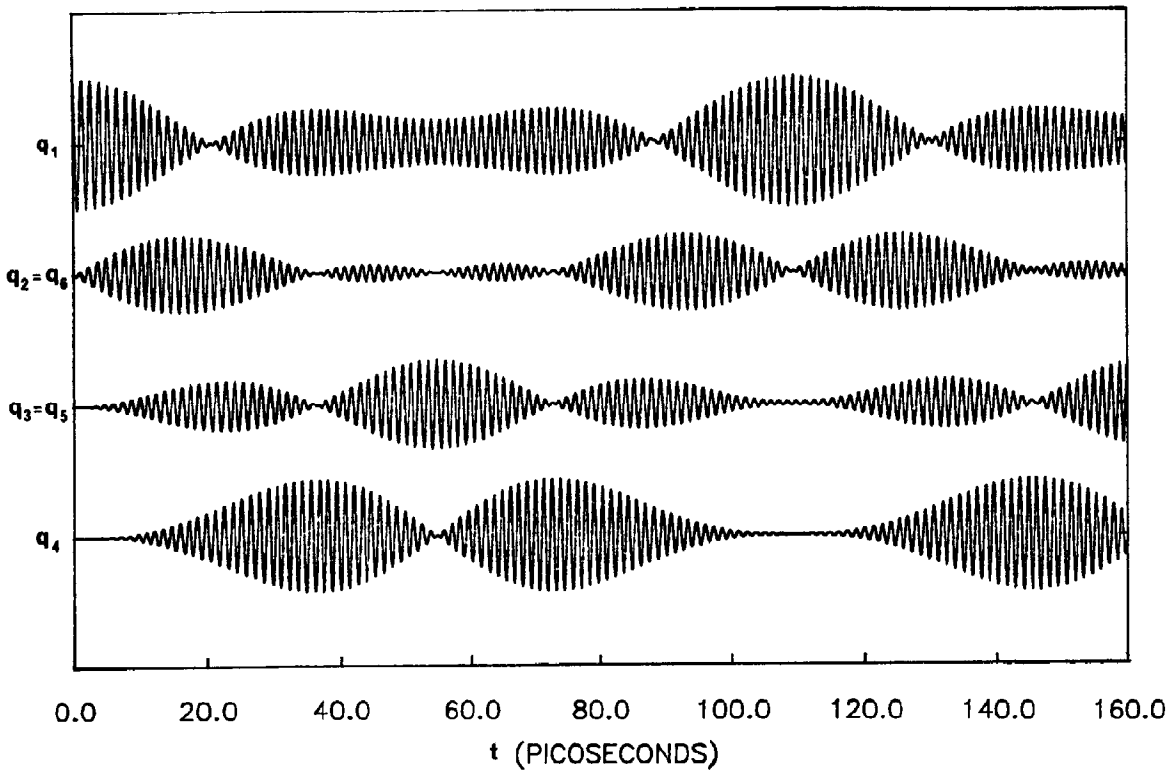

Fig. 13. Plot of q_1, $q_2 = q_6$, $q_3 = q_5$ and q_4 vs. t (see eq. 41) when $x = 0.1$, $\omega_0 = 4.71 \times 10^{12}$/s (i.e., $\bar{\nu}_0 = 25$ cm^{-1}).

From eqs. 42 and 43 we have

$$
\begin{cases}
\begin{cases} \max|q_1| = A, \quad \text{when } t = 16l\pi/x\omega_0 \\ \min|q_1| = 0, \\ \quad \text{when } t = 8\{2l\pi \pm \cos^{-1}[(\sqrt{3}-1)/2]\} \\ \qquad /x\omega_0 \simeq 8(2l \pm 0.38)\pi/x\omega_0 \end{cases} \\
\begin{cases} \max|q_2| = \max|q_6| \simeq 0.59A, \\ \quad \text{when } t \simeq 8\{2l\pi \pm \cos^{-1}[(\sqrt{33}-1)/8]\}/x\omega_0 \\ \qquad \simeq 8\,(2l + 0.30)\pi/x\omega_0 \\ \min|q_2| = \min|q_6| = 0, \\ \quad \text{when } t = 8l\pi/x\omega_0 \text{ or } 8(2l \pm 2/3)\pi/x\omega_0 \end{cases} \\
\begin{cases} \max|q_3| = \max|q_5| = \frac{2}{3}A \simeq 0.67A, \\ \quad \text{when } t = 8\,(2l + 1)\pi/x\omega_0 \\ \min|q_3| = \min|q_6| = 0, \\ \quad \text{when } t = 16l\pi/x\omega_0 \text{ or } 8(2l \pm 2/\sqrt{3})\pi/x\omega_0 \end{cases} \\
\begin{cases} \max|q_4| = \sqrt{3}/2A \simeq 0.87A, \\ \quad \text{when } t = 8(2l \pm 2/\sqrt{3})\pi/x\omega_0 \\ \min|q_4| = 0, \\ \quad \text{when } t = 8l\pi/x\omega_0 \end{cases} \\
(l = 0, 1, 2, \ldots;\ t \geq 0)
\end{cases}
\tag{44}
$$

Therefore, we have

$$
\frac{\max E_1}{1} \simeq \frac{\max E_2}{0.35} \simeq \frac{\max E_3}{0.45} \simeq \frac{\max E_4}{0.76} \simeq \frac{\max E_5}{0.45} \simeq \frac{\max E_6}{0.35} \tag{45}
$$

which clearly indicates that, after the first subunit is excited, the maximum energies transmitted to the second and sixth (close adjacent) subunits are smaller than those to the third and fifth (next adjacent) subunits, while the maximum energies transmitted to the third and fifth subunits are smaller than that to the fourth (diagonal) subunit, as can also been seen from the peaks drawn in fig. 13. Consequently, for a protein hexamer with a hexagonal arrangement, after a ligand binds to a subunit, its diagonal subunit will be activated more efficiently so as to possess a greater probability of binding with the next ligand. It should be realized, however, that fig. 13 also includes the contributions from the higher-order terms of x. Therefore,

after the first slow period, i.e., $t > T = 16\pi/x\omega_0 \simeq$ 106.7 ps, the maximum peaks decrease slightly whereas the minimum peaks increase slightly, as shown in fig. 13. Such a dispersion phenomenon will gradually become visible after a few slow periods, as more distinctly shown in fig. 9 where the slow period is much shorter (i.e., $T = 4\pi/x\omega_0$ $\simeq$ 26.6 ps only) and hence the dispersion phenomenon is more conspicuous within the same time interval.

Furthermore, from eq. 43 we obtain (cf. eq. 18):

$$\begin{cases} T^{1\to 2} = T^{1\to 6} = 2.4\pi/x\omega_0 = 1.2xc\tilde{\nu}_0 \\ T^{1\to 3} = T^{1\to 5} = 8\pi/x\omega_0 = 4/xc\tilde{\nu}_0 \\ T^{1\to 4} = 16\pi/3x\omega_0 = 8/3xc\tilde{\nu}_0 = 2.7/xc\tilde{\nu}_0 \end{cases} \quad (46)$$

If $\tilde{\nu}_0 = 25\ \mathrm{cm}^{-1}$ [4], $x = 0.1$, then we have $T^{1\to 2} = T^{1\to 6}$ 16 ps, $T^{1\to 3} = T^{1\to 5} = 52$ ps, and $T^{1\to 4} =$ 35 ps, respectively. Therefore, the lower time limit of cooperative transmission will be different for different couples of subunits.

5. Some remarks

This section is devoted to answering some skeptical questions which might be raised concerning the validity of the present model.

First, the model used here is an ideal model without considering any dissipative effects. Any vibration in a real protein oligomer will involve dissipation. Will it completely invalidate the physical picture presented based on such an ideal model? Indeed, for any real system owing to dissipation of energy by the environment (damping), the intensity of motion will decrease with time. This, however, will not destroy the basic feature of the alternating behavior of the amplitudes as described here, provided that the damping is not exceedingly large [31]. In other words, the basic physical picture of energy transmission via the resonance-coupled mechanism will still remain approximately valid at least for the initial few periods, which are only interesting for our present purpose. This is very similar to the cases in real life where people often experience various resonance effects no matter how complicated the real environments are. This is also somewhat like the fact that an outstanding low-frequency normal mode, the so-called dominant low-frequency mode, can always be observed for many protein molecules [1,2,4,5] although various extremely complicated dissipative effects certainly do exist in a biological macromolecule. Therefore, the quintessence of the present theory will still hold true even if some complicated factors such as the 'frictional' interaction inside a protein molecule [7] and the solvent viscosity are taken into account.

Second, what will one find when comparing the predicted lower time limit of allosteric transition with experiment? To answer this question, we should first realize the following point. The lower time limit is based on the period characterizing the energy flow from one subunit to the other via a resonance-coupled mechanism. This kind of energy transmission will somehow trigger a conformational change in another subunit when its energy reaches the maximum through such an accumulated process of energy flow. But it should always be kept in mind that the conformational change itself also takes time even after being triggered because it involves some kind of rearrangement in structure. In other words, the total time of an allosteric transition should be the sum of these two types of time. Therefore, it should not be surprising at all if the lower time limit thus defined is smaller than the time for the whole allosteric process. This is somewhat like the diffusion-controlled reaction in enzyme kinetics, where all the reaction rates must be smaller than their diffusion limits [34–36]. Similarly, according to the concept of the resonance-controlled trigger as introduced in section 4, except for some very extreme cases in which the time for the rearrangement in structure is zero (which is actually too extreme to exist) after being triggered, the whole allosteric transition must take longer (or much longer if the time for such a rearrangement is much larger) than the corresponding lower time limit as defined here. Indeed, to our knowledge thus far none of the experimental data found to be able to represent the time scale of an allosteric process can exceed such a lower time limit of 5–50 ps as estimated here, fully indicating a logical consistency between our theory and experiments.

6. Conclusion

Low-frequency resonance plays a central role in the energy transmission during the cooperative interaction of subunits in a protein oligomer [12]. Such a deduction is further quantitatively demonstrated by the mathematical theory developed in the present paper. According to the calculated results, it is predicted that, for protein oligomers with a polygon arrangement, the energy transmission between two diagonal subunits via such a resonance mechanism is the most efficient, implying that, after one subunit of this kind of protein oligomer is bound to a ligand, its diagonal subunit will possess the greatest cooperative effect in comparison with the other subunits. Moreover, according to the concept of the resonance-controlled trigger developed from the present theory, it is also possible in principle to estimate the lower time limit of the allosteric transition for a given protein oligomer.

Acknowledgement

Illuminating discussion at Kyoto University, Japan, with Professor Tatsuo Ooi is gratefully acknowledged.

Appendix

Here let us derive the general solutions as given by eqs. 7–10. Substituting

$$q_i = C_i \cos(\omega t + \phi) \tag{A1}$$

into eq. 4, we obtain

$$\begin{bmatrix} a_{11}-\omega^2 & a_{12} & \dots & a_{1n} \\ a_{21} & a_{22}-\omega^2 & \dots & a_{2n} \\ \vdots & \vdots & & \vdots \\ a_{n1} & a_{n2} & \dots & a_{nn}-\omega^2 \end{bmatrix} \begin{bmatrix} C_1 \\ C_2 \\ \vdots \\ C_n \end{bmatrix} = 0 \tag{A2}$$

where the relation of ω and C_i with the ω_l and C_{il} in eq. 7 is as follows. As is well known, the non-trivial solution of the above equation requires

$$\det(\boldsymbol{A} - \omega^2 \boldsymbol{I}) = 0 \tag{A3}$$

where

$$\boldsymbol{A} = \begin{bmatrix} a_{11} & a_{12} & \dots & a_{1n} \\ a_{21} & a_{22} & \dots & a_{2n} \\ \vdots & \vdots & & \vdots \\ a_{n1} & a_{n2} & \dots & a_{nn} \end{bmatrix} \tag{A4}$$

and $\boldsymbol{I}$ is the unitary matrix. Therefore, ω_l ($l = 1, 2, \dots, n$) is the lth root of the ω obtained by solving eq. A2, and C_{il} the C_i obtained by substituting ω_l into eq. A1.

According to eq. 6, the matrix $\boldsymbol{A}$ can be further simplified to

$$\boldsymbol{A} = \begin{bmatrix} b_1 & b_2 & b_3 & \dots & b_n \\ b_n & b_1 & b_2 & \dots & b_{n-1} \\ \vdots & \vdots & \vdots & & \vdots \\ b_2 & b_3 & b_4 & \dots & b_1 \end{bmatrix}$$

$$= b_1 \begin{bmatrix} 1 & & & & \\ & 1 & & & \\ & & \ddots & & \\ & & & & 1 \\ & & & 1 & \end{bmatrix} + b_2 \begin{bmatrix} 0 & 1 & & & \\ & & 1 & & \\ & & & \ddots & \\ & & & & 1 \\ 1 & & & & 0 \end{bmatrix} + \dots$$

$$+ b_3 \begin{bmatrix} 0 & 0 & 1 & & \\ & & & 1 & \\ & & & & \ddots \\ & & & & 1 \\ 1 & & & & 0 \\ 0 & 1 & & & 0 \end{bmatrix} + b_n \begin{bmatrix} 0 & & & & 1 \\ 1 & & & & \\ & 1 & & & \\ & & \ddots & & \\ & & & 1 & 0 \end{bmatrix} \tag{A5}$$

where b_i ($i = 1, 2, \dots, n$) are given by eq. 5 subject to the condition, eq. 6, i.e., they can be explicitly expressed by eq. 9. Suppose [37–39]:

$$\boldsymbol{D} = \begin{bmatrix} 0 & 1 & & & \\ & & 1 & & \\ & & & \ddots & \\ & & & & 1 \\ 1 & & & & 0 \end{bmatrix} \tag{A6}$$

it then follows that

$$\boldsymbol{A} = b_1\boldsymbol{I} + b2_2\boldsymbol{D} + b_3\boldsymbol{D}^2 + \ldots + b_n\boldsymbol{D}^{n-1} \qquad \text{(A7)}$$

Solving the equation

$$\boldsymbol{D}\begin{bmatrix} C_1 \\ C_2 \\ \vdots \\ C_n \end{bmatrix} = \lambda \begin{bmatrix} C_1 \\ C_2 \\ \vdots \\ C_n \end{bmatrix} \qquad \text{(A8)}$$

we obtain

$$\lambda_l = e^{i(2l\pi/n)} \quad (l = 1, 2, \ldots, n) \qquad \text{(A9)}$$

and

$$\boldsymbol{C}_l = \begin{bmatrix} C_1 \\ C_2 \\ \vdots \\ C_n \end{bmatrix}_l = \begin{bmatrix} 1 \\ e^{i(2l\pi/n)} \\ \vdots \\ e^{i[2l(n-1)]\pi/n} \end{bmatrix} \qquad \text{(A10)}$$

We now have

$$\boldsymbol{A}\begin{bmatrix} C_1 \\ C_2 \\ \vdots \\ C_n \end{bmatrix}_l = \left(b_1\boldsymbol{I} + b_2\boldsymbol{D} + b_3\boldsymbol{D}^2 + \ldots + b_n\boldsymbol{D}^{n-1}\right)\begin{bmatrix} C_1 \\ C_2 \\ \vdots \\ C_n \end{bmatrix}_l$$

$$= \left(b_1 + b_2\lambda_l + b_3\lambda_l^2 + \ldots + b_n\lambda_l^{n-1}\right)\begin{bmatrix} C_1 \\ C_2 \\ \vdots \\ C_n \end{bmatrix}_l$$

$$= \omega_l^2 \begin{bmatrix} C_1 \\ C_2 \\ \vdots \\ C_n \end{bmatrix}_l \qquad \text{(A11)}$$

Consequently, the eigenvalues of $\boldsymbol{A}$ are (cf. eq. A2):

$$\omega_l^2 = b_1 + b_2e^{i(2l\pi/n)} + b_3e^{i(4l\pi/n)} + \ldots + b_ne^{i[2l(n-1)\pi/n]}$$
$$(l = 1, 2, \ldots, n) \qquad \text{(A12)}$$

and the corresponding eigenvectors are the same as those of $\boldsymbol{D}$ as given by eq. A10.

Furthermore, because of $k_{ij} = k_{ji}$, $\boldsymbol{A}$ must also be a symmetric matrix, which means that

$$b_2 = b_n,$$

$$b_3 = b_{n-1}, \ldots, \begin{cases} b_{n/2} = b_{(n+4)/2} & \text{if } n \text{ is even} \\ b_{(n+1)/2} = b_{(n+3)/2} & \text{if } n \text{ is odd} \end{cases} \qquad \text{(A13)}$$

On the other hand, according to the property of $\boldsymbol{D}$, we have $\boldsymbol{D}^{n-i} = \boldsymbol{D}^{-i}$. Therefore, $\boldsymbol{A}$ can be expressed as

$$\boldsymbol{A} = b_1\boldsymbol{I} + b_2(\boldsymbol{D} + \boldsymbol{D}^{-1}) + b_3(\boldsymbol{D}^2 + \boldsymbol{D}^{-2}) + \ldots$$
$$+ \begin{cases} b_{(n/2)+1}\boldsymbol{D}^{n/2} & \text{if } n \text{ is even} \\ b_{(n+1)/2}(\boldsymbol{D}^{(n-1)/2} + \boldsymbol{D}^{-(n-1)/2}) & \text{if } n \text{ is odd} \end{cases} \qquad \text{(A14)}$$

Consequently, eq. A12 can be further expressed in terms of real values as shown in eq. 8. Moreover, it is easy to see from eq. 8 that $\omega_l^2 = \omega_{n-l}^2$; i.e., the eigenvalue is double degenerate except for $l = n/2$ and n. Accordingly, the corresponding eigenvectors can also be expressed as real values in terms of some linear combination such as $(\boldsymbol{C}_l + \boldsymbol{C}_{n-l})/2$ and $(\boldsymbol{C}_l - \boldsymbol{C}_{n-l})/2$ as finally given by eq. 10.

The general solution of eq. 4 should be a linear summation of the n special solutions for q_i, corresponding to n eigenvalues of ω_i, and hence should eventually be given by eq. 7.

References

1 K.G. Brown, S.C. Erfurth, E.W. Small and W.L. Peticolas, Proc. Natl. Acad. Sci. U.S.A. 69 (1972) 1467.
2 L. Genzel, F. Keilman, T.P. Martin, G. Winterling, Y. Yacoby, H. Fröhlich and M.W. Makinen, Biopolymers 15 (1976) 219.
3 P.C. Painter, L.E. Mosher and C. Rhoads, Biopolymers 20 (1981) 243.
4 P.C. Painter, L.E. Mosher and C. Rhoads, Biopolymers 21 (1982) 1469.
5 G.J. Evans, M.W. Evans and R. Pething, Spectrochim. Acta 38A (1982) 421.
6 Y. Suezaki and N. Gō, Int. J. Peptide Protein Res. 7 (1975) 333.
7 K.C. Chou, Biochem. J. 209 (1983) 573.
8 K.C. Chou, Biochem. J. 215 (1983) 465.
9 N. Gō, T. Noguti and T. Nishikawa, Proc. Natl. Acad. Sci. U.S.A. 80 (1983) 3696.
10 K.C. Chou, Biophys. J. 45 (1984) 881.
11 K.C. Chou, Biochem. J. 221 (1984) 27.

12 K.C. Chou, Biophys. Chem. 20 (1984) 61.
13 K.C. Chou, Int. J. Biol. Macromol. 7 (1985) 77.
14 D.E. Green, Ann. N.Y. Sci. 227 (1974) 6.
15 S. Ji, Ann. N.Y. Sci. 227 (1974) 419.
16 H. Fröhlich, Proc. Natl. Acad. Sci. U.S.A. 72 (1975) 4211.
17 K.C. Chou and N.Y. Chen, Sci. Sin. (English Edn.) 20 (1977) 447.
18 K.C. Chou and N.Y. Chen, Huaxue Tongbao (Chinese edn.) 5 (1978) 29.
19 G. Careri, P. Fasella and E. Gratton, CRC Crit Rev. Biochem. 3 (1975) 141.
20 S.W. Englander, Comments Mol. Cell. Biophys. 1 (1980) 15.
21 K.C. Chou, N.Y. Chen and S. Forsén, Chem. Scr. 18 (1981) 126.
22 G.P. Zhou, Shengwu Huaxue Yu Shengwu Wulin Jinzhan (Chinese edn.) 5 (1981) 19.
23 H.M. Sobell, A. Banerjee, E.D. Lozansky, G.P. Zhou and K.C. Chou, in: Structure and dynamics: nucleic acids and proteins, eds. E. Clementi and R.H. Sarma (Adenine Press, New York, 1983) p. 181.
24 T. Svedberg and R. Fahraeus, J. Am. Chem. Soc. 48 (1926) 430.
25 T. Svedberg, Nature 123 (1929) 871.
26 J.C. Gerhart and A.B. Pardee, J. Biol. Chem. 237 (1963) 891.
27 J. Monod, J. Wyman and J.P. Changeux, J. Mol. Biol. 12 (1965) 88.
28 D.E. Koshland Jr., G. Nemethy and D. Filmer, Biochemistry 5 (1966) 365.
29 I.M. Klotz, N.R. Langerman and D.W. Darnall, Annu. Rev. Biochem. 39 (1970) 25.
30 M.F. Perutz, Proc. Roy. Soc. B173 (1969) 113.
31 P.L. Luisi and M. Zandomeneghi, Biophys. Chem. 1 (1974) 358.
32 S.A. Bernhard, M.F. Dunn, P.L. Luisi and P. Schack, Biochemistry 9 (1970) 185.
33 W.B. Stallcup and D.E. Koshland Jr, Biochem. Biophys. Res. Commun. 49 (1972) 1108.
34 K.C. Chou and S.P. Jiang, Sci. Sin. (English edn.) 17 (1974) 664.
35 G.Q. Zhou and W.Z. Zhong, Eur. J. Biochem. 128 (1982) 383.
36 G. Zhou, M.T. Wong and G.Q. Zhou, Biophys. Chem. 18 (1983) 125.
37 A.C. Tang and Y.S. Kiang, Sci. Sin. (English edn.) 20 (1977) 595.
38 A.C. Tang and Y.S. Kiang, Sci. Sin. (English edn.) 19 (1976) 207.
39 Y.S. Kiang, Int. J. Quantum Chem. 18 (1980) 331.
40 K.C. Chou, Biophys. J. 48 (1985) in the press.